remote sensing

MDPI

Article

Non-Destructive Estimation of Deciduous Forest Metrics: Comparisons between UAV-LiDAR, UAV-DAP, and Terrestrial LiDAR Leaf-Off Point Clouds Using Two QSMs

Yi Gan [1], Quan Wang [2,*] and Guangman Song [2]

[1] Graduate School of Science and Technology, Shizuoka University, Shizuoka 422-8529, Japan; gan.y.19@shizuoka.ac.jp
[2] Faculty of Agriculture, Shizuoka University, Shizuoka 422-8529, Japan; song.guangman@shizuoka.ac.jp
* Correspondence: wang.quan@shizuoka.ac.jp; Tel.: +81-54-2383683

Abstract: Timely acquisition of forest structure is crucial for understanding the dynamics of ecosystem functions. Despite the fact that the combination of different quantitative structure models (QSMs) and point cloud sources (ALS and DAP) has shown great potential to characterize tree structure, few studies have addressed their pros and cons in alpine temperate deciduous forests. In this study, different point clouds from UAV-mounted LiDAR and DAP under leaf-off conditions were first processed into individual tree point clouds, and then explicit 3D tree models of the forest were reconstructed using the TreeQSM and AdQSM methods. Structural metrics obtained from the two QSMs were evaluated based on terrestrial LiDAR (TLS)-based surveys. The results showed that ALS-based predictions of forest structure outperformed DAP-based predictions at both plot and tree levels. TreeQSM performed with comparable accuracy to AdQSM for estimating tree height, regardless of ALS (plot level: 0.93 vs. 0.94; tree level: 0.92 vs. 0.92) and DAP (plot level: 0.86 vs. 0.86; tree level: 0.89 vs. 0.90) point clouds. These results provide a robust and efficient workflow that takes advantage of UAV monitoring for estimating forest structural metrics and suggest the effectiveness of LiDAR in temperate deciduous forests.

Keywords: airborne laser scanning; terrestrial laser scanning; digital aerial photogrammetry; forest structure; TreeQSM; AdQSM

Citation: Gan, Y.; Wang, Q.; Song, G. Non-Destructive Estimation of Deciduous Forest Metrics: Comparisons between UAV-LiDAR, UAV-DAP, and Terrestrial LiDAR Leaf-Off Point Clouds Using Two QSMs. *Remote Sens.* **2024**, *16*, 697. https://doi.org/10.3390/rs16040697

Academic Editors: Francesca Ardizzone, Gabriella Caroti and Yuankun Xu

Received: 18 January 2024
Revised: 10 February 2024
Accepted: 12 February 2024
Published: 16 February 2024

1. Introduction

Traditional forest inventories have often relied on ground surveys of specific sample plots, which are costly, labor-intensive, and spatially limited [1,2]. In comparison, recent point cloud technology, derived from advanced remote sensing approaches such as photogrammetry and light detection and ranging (Li-DAR), has opened new avenues for automating and improving the accuracy of forest inventory assessments in a rapid and non-destructive manner [3–5], enabling more accurate and timely assessments of forest resources for precise forest management.

Point cloud technology provides a three-dimensional representation of forest structure and captures a wealth of detailed information associated with forest structure, such as tree height, basal area, canopy density, and gap fraction [6,7]. The acquisition platforms that enable the collection of point clouds and the inference methods derived from them are of paramount importance in the extraction of forest structure.

The point clouds derived from different techniques and platforms, especially terrestrial laser scanning (TLS), airborne laser scanning (ALS), and digital aerial photogrammetry (DAP), have been widely used in the extraction of forest structure [3,8,9]. Among them, ALS has been the primary data source for deriving forest structural characteristics [10–13]. However, ALS for individual tree segmentation could introduce errors [14,15], and ALS could better estimate forest density with respect to taller trees, while leading to underestimation

of smaller trees [16]. Alternatively, digital aerial photography (DAP) shows great potential for deriving forest structural metrics [17–20]. It has been shown to provide predictive ability comparable to that of ALS data [20,21], but with lower data acquisition costs [22,23]. On the other hand, TLS acquires high-density point clouds from the ground up and has made significant progress in accurately measuring forest structural attributes [4,24], such as stem volume, crown structure, and leaf angle distribution [25–27]. In general, TLS can provide high-resolution data with less noise [8], and is able to map structurally complex forests and detect fine-scale internal features within the canopy, making it useful for validating ALS data [28,29].

Meanwhile, point cloud derivation approaches are the next crucial step in forest structure extraction, which can be broadly categorized into the voxel-based approach [30–32] and geometric modeling [33,34]. The voxel-based method considers the downsampling of the original point clouds and generally relocates the points into regular cubics with different approaches [8,35,36] to estimate structures [37,38], and the estimation accuracy is influenced by the voxel size [30,39,40]. In comparison, geometric modeling allows explicit reconstruction of individual tree structures modeled by quantitative structure modeling (QSM) based on tree segmentation. In recent years, it has been increasingly recognized to create explicit 3D models of trees for tree structure assessment [41,42], providing highly detailed tree attributes for biomass estimation and other purposes [43–46].

There are some established approaches for reconstructing QSMs, such as TreeQSM [42], SimpleTree [47], and AdQSM [48], to name a few. TreeQSM has been successfully applied to extract structural attributes such as branch diameter and length estimation [44] and stem biomass assessment in forest scenarios [49]. Recently, a new QSM algorithm (AdQSM) has been released and successfully applied to quantitative structure modeling of tropical trees from TLS point clouds for above-ground biomass (AGB) estimation [48]. However, the two QSMs have mostly taken the TLS-based point clouds as input and produced good results [44,50–53], but fewer evaluations have been made on the point clouds from other sources, despite the increasing number of studies using ALS-based point clouds. Among the few, Brede et al. [41] evaluated tree volume using a QSM based on unmanned aerial vehicle laser scanning data and found that concordance was influenced by denser stands and smaller branches. Similarly, Ye et al. [54] evaluated the potential of UAV-based DAP point clouds as an input to a QSM for estimating woody biomass, but claimed that QSMs cannot show good performance with UAV data. To the best of our knowledge, DAP point clouds as input to QSMs have not been explored yet. Therefore, the applications of the two QSM methods on point clouds from different sources should be comprehensively investigated.

The overall objective of this study is to perform a comprehensive comparison of the non-destructive estimation of structural metrics from TreeQSM and AdQSM tree models using point cloud data from ALS, DAP, and TLS data sources in a complex alpine temperate deciduous forest. Specifically, this study aims to (1) compare the accuracy of ALS and DAP point clouds in estimating forest structural metrics with reference to TLS point clouds; and (2) evaluate the performance of TreeQSM and AdQSM approaches for estimating forest structural attributes based on the different data sources. The comprehensive investigation conducted in this study is useful for biomass and other functional assessments, and also provides a foundation for other forest types included in related studies.

2. Materials and Methods

2.1. Study Site and Ground Truth Data

Seven plots in the Shizuoka University Forest in Nakakawane, Japan were the study sites in this study. These seven plots were selected based on a trade-off between the number of trees and labor intensity. All the plots were adjacent to each other and each occupied an area of 20 m $\times$ 20 m. The predominant forest type of the study area was temperate deciduous forest, with an average annual precipitation and temperature of approximately 2153 mm and 17 °C, respectively [55,56].

The TLS-based metrics served as the ground truth data in this study. A FARO Focus3D × 130 3D single-return scanner (FARO, Lake Mary, FL, USA) was used to obtain raw TLS point clouds under leaf-off conditions. The scanner carries an optical transmitter with a wavelength of 1550 nm, and the beam divergence and sampling angular step size are typically 0.19 mrad (0.011°) and 0.009°, respectively. The field of view angles for vertical and horizontal are 0°–300° and 0°–360°, respectively. TLS measurements for seven plots were performed on 4 December 2023. Because the scanner operates exclusively in single-return mode, multiple scans were performed on each plot to collect comprehensive real-world scenes. The complete seven plots were scanned from 18 locations, resulting in 18 individually scanned point clouds (Figure 1).

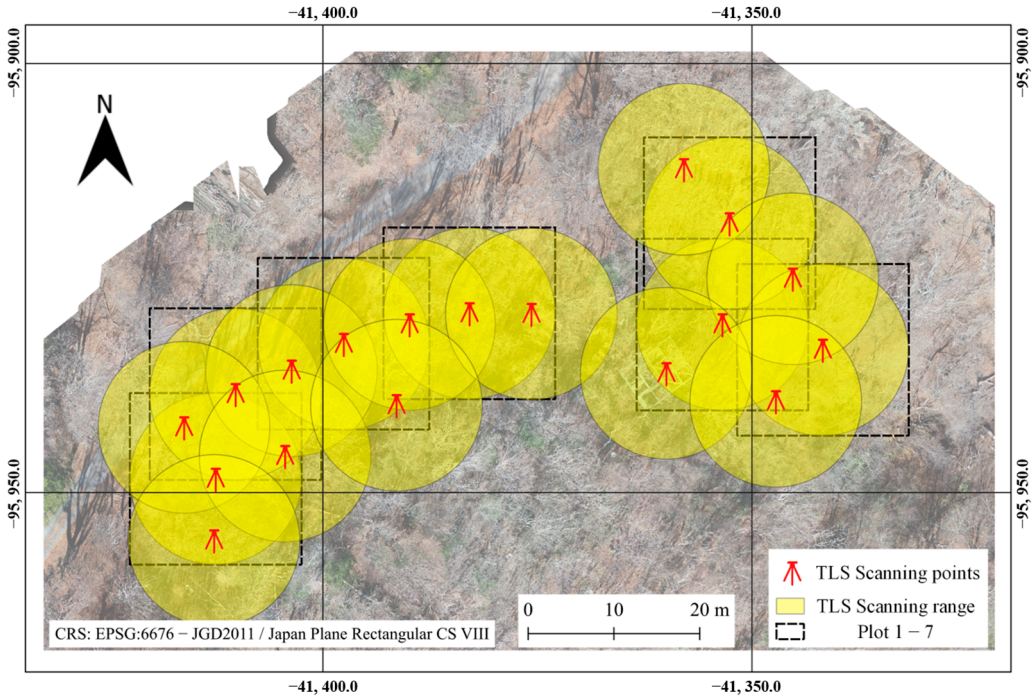

Figure 1. Locations of the plots and TLS scans within the study site.

Raw TLS point clouds were filtered and exported in SCENE software (version 6.2.4.30, FARO, Lake Mary, FL, USA). GlobalMatch [57] was employed to carry out point cloud registration at the plot level by calculating a 4 by 4 transformation matrix. Point cloud merging and cropping was conducted with CloudCompare software (version 2.13.beta). The Computree platform (version 5.0, ONF, Paris, France) and the plug-in SimpleForest [58] were employed for individual tree point cloud segmentation. TreeQSM (version 2.4.1, Raumonen et al. [42]) was further applied for quantitative structure modeling and structural metrics calculation. In total, 150 trees within 7 plots were processed and served as ground truth data. Figure 2 shows the distributions and statistics of representative structural metrics from TLS point clouds, including diameter at breast height (DBH), tree height (H), and crown area (CA).

2.2. UAV-Based Measurements and Pre-Processing

The UAV-based measurements were performed on the same day as the TLS measurements. Both ALS and DAP data were collected using the sensors carried by the DJI Matrice 300 RTK (DJI, Shenzhen, China). Specifically, ALS data were collected using a DJI Zenmuse L1 LiDAR scanning system (DJI, Shenzhen, China), which has a horizontal accuracy of 0.1 m per 50 m and a vertical accuracy of 0.05 m (standard deviation). The measurement beam divergence of the scanner was set to 0.28° in the vertical plane and 0.03° in the horizontal plane, allowing up to 3 reflections per laser beam in multiple-return mode. The DAP data were captured using a DJI Zenmuse P1 digital photography camera (DJI,

Shenzhen, China), which has a superior resolution of 45 megapixels, producing images of 8192 × 5490 pixels.

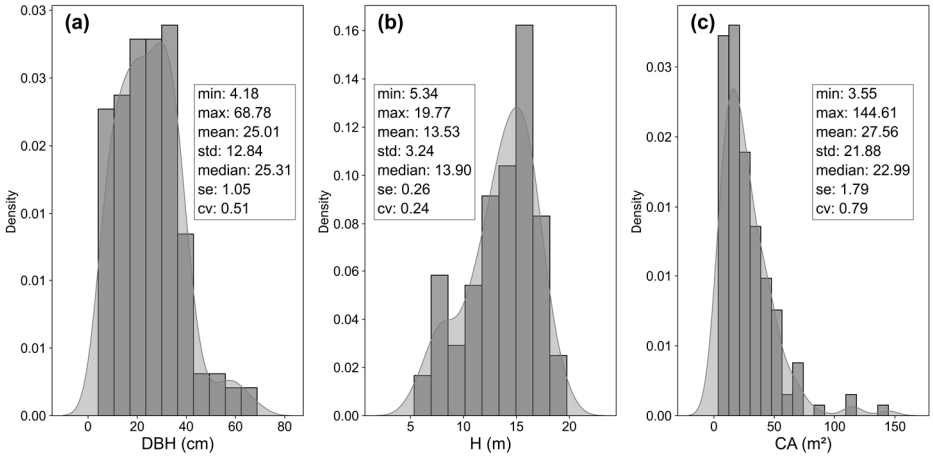

Figure 2. The distribution and statistics of structural metrics calculated by TreeQSM based on TLS point clouds, including DBH (**a**), H (**b**), and CA (**c**).

Automatically programmed with DJI Pilot, the flight patterns of forward and lateral overlap ratio were set to 70% and 80%, respectively, with an altitude of 60 m above the relative launch point and IMU calibration enabled when performing ALS measurements. The return mode was set to triple, the sampling rate was set to 160 KHz, and the scan mode was set to non-repetitive with RGB coloring enabled. The expected point cloud density and ground sampling distance (GSD) were 1789 point/m^2 and 1.64 cm/pixel, respectively. To ensure the precision of the UAV flight and data acquisition, the DJI D-RTK 2 high-precision GNSS mobile station (DJI, Shenzhen, China) was used to acquire the precise position information of the drones in three-dimensional space.

Raw scanning data were subsequently input to DJI TERRA 3.5.5 (DJI, Shenzhen, China) for post-processing, and process parameters were set to high quality. The exported ALS and DAP point clouds were clipped into rectangular cuboids with dimensions of 20 m in length and width using CloudCompare software (version 2.13.beta) for further analysis.

2.3. Tree Segmentation

A bottom-up method for tree segmentation was implemented in the Computree platform with the SimpleForest plug-in. Specifically, the plot point clouds were separated into ground and vegetation points; ground points were used to construct a digital terrain model (DTM); seed points for segmentation were specified by cutting the vegetation points over the DTM with multiple specific heights; a Dijkstra segmentation method was implemented for individual tree point segmentation by combining the seed points and vegetation points. The parameters used during the segmentation process were not consistent and changed frequently, depending on the variations in data sources and real-world scenarios. In total, 108 and 23 trees were successfully segmented from seven ALS and DAP point clouds, respectively. The tree segmentation workflow used in this study is shown in Figure 3.

2.4. Quantitative Structure Modeling

TreeQSM (Raumonen et al. [42], https://github.com/InverseTampere/TreeQSM, latest accessed on 1 January 2024) and AdQSM (Fan et al. [48], https://github.com/GuangpengFan/AdQSM, latest accessed on 2 January 2024) were selected for modeling the segmented ALS and DAP tree point cloud data in this study. The structural metrics were automatically calculated upon the completion of modeling, and common structural metrics output from TreeQSM and AdQSM are shown in Table 1.

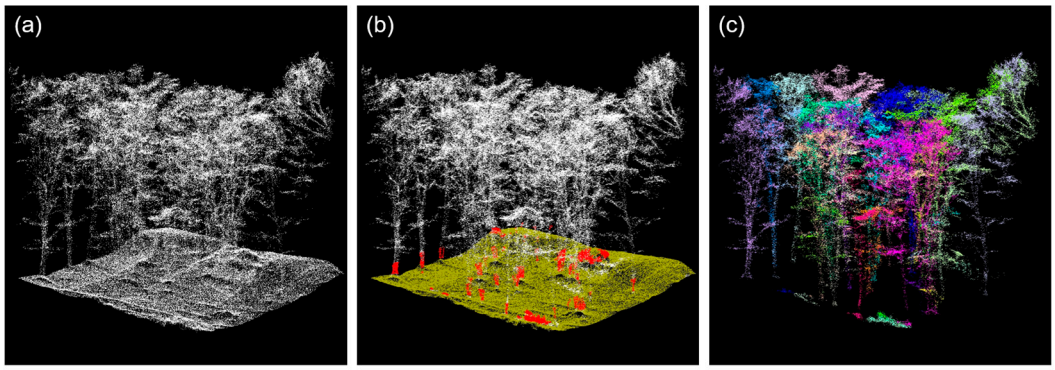

Figure 3. Segmentation process of individual trees from ALS/DAP point clouds. (**a**) Raw point cloud data; (**b**) classified ground (brown), vegetation (white), and seed points (red); (**c**) segmented individual tree points by Dijkstra segmentation algorithm with different colors represented.

Table 1. Common structural metrics in TreeQSM and AdQSM.

Category	Attribute	Description
Length	DBH	The diameter of the cylinder in the QSM at the right height
	TreeHeight	Height (m) of the tree
	TrunkLength	Length (m) of the stem
	CrownLength	Crown's vertical length (m)
	TrunkArea	Total surface area (m^2) of the stem
	CrownBaseHeight	The crown's base height (m) from the ground
Area	BranchArea	Total surface area (m^2) of the branches
	TrunkArea	Total surface area (m^2) of the trunk
	TotalArea	Total surface area (m^2) of the tree
	CrownAreaAlpha	Area (m^2) of the crown's planar projection's alpha shape
	CrownAreaConv	Area (m^2) of the crown's planar projection's convex hull
Volume	TrunkVolume	The total volume (L) of the stem part
	BranchVolume	The total volume (L) of the branch part
	TotalVolume	The total volume (L) of the tree
	CrownVolumeAlpha	Total volume (L) of the crown's alpha shape
	CrownVolumeConv	Total volume (L) of the crown's convex hull
Other	Number of branches	Number of branches

TreeQSM has been successfully used for the estimation of biophysical parameters since it considers the tree's inherent structure [41,52]. The detailed 3D reconstructions of the branch and stem architecture for each tree followed the workflow outlined in the study of Calders et al. [52]. In TreeQSM, three critical parameters affect model reconstruction: PatchDiam1, PatchDiam2Min, and PatchDiam2Max. Following the TreeQSM version 2.4.1 instructions, we configured these parameters with 2, 3, and 2 values, respectively, resulting in a total of 12 different parameter combinations for model reconstruction. Each of these combinations was reconstructed five times, leading to the generation of 60 models for a single tree point cloud. To select the best model from the aforementioned 60 models, we utilized the cylinder distance metrics, specifically "trunk+branch_mean_dis," for optimized model selection.

AdQSM is a new tree quantitative structure model (QSM) developed based on the AdTree algorithm [59]. This QSM is capable of reconstructing individual tree structure models by applying not only TLS point cloud data but also ALS point cloud data. Height segmentation (HS) and cloud parameter (CP) serve as two critical parameters to control the quantitative structure modeling process. In this study, following the author's recommendations in the manual, the CP was kept at its default value of 0.003 and was not changed for each reconstruction. By setting different values of HS for multiple reconstructions (0.4, 0.6,

0.8, 1.0), the average value of each structure parameter was calculated as the final result of the tree reconstruction.

2.5. Analysis Flowchart

The overall workflow of data processing steps in this study is shown in Figure 4. Highly detailed TLS data were treated as ground truth to evaluate the performance of UAV-based ALS and DAP point cloud data in forest structural metrics estimation, including field measurements, tree segmentation, quantitative structure modeling, and structure metrics evaluation. Specifically, ground-based and UAV-based measurements were performed to obtain raw TLS, ALS, and DAP data, and corresponding point cloud data were exported after several pre-processing steps. These point clouds were then segmented into individual tree point clouds using the bottom-up method under the SimpleForest plug-in mounted on Computree. Then, the two QSM methods were performed to generate the quantitative structure model of each tree; the structural metrics are automatically calculated when the QSM modeling is completed. Finally, the structural metrics of DBH, H, and CA were selected as evaluation indicators, and the accuracy and model performance of structural metrics estimated from ALS and DAP data were evaluated by TLS data. The statistical measures of the coefficient of determination (R^2) and root mean square error (RMSE) were used to evaluate their predictive accuracy.

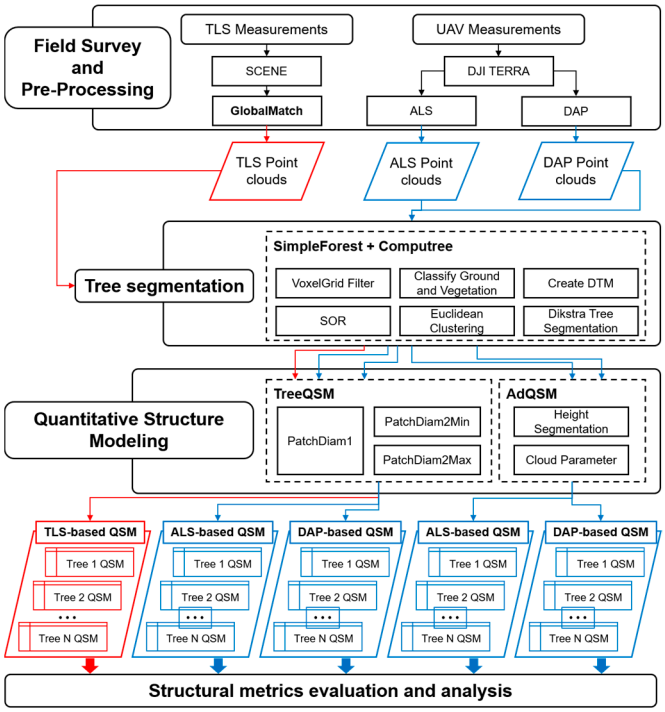

Figure 4. Flowchart of the overall process in this study.

3. Results

3.1. ALS Point Cloud-Based QSM Estimations: TreeQSM vs. AdQSM

Plot-level statistical descriptions of forest structural metrics, derived from ALS data using TreeQSM and AdQSM, are presented in Figure 5. For TreeQSM results across the seven plots, the mean values of DBH, H, and CA varied from 27.97 to 39.84 cm, 14.04 to 16.56 m, and 24.78 to 44.40 m^2, respectively. Concurrently, the standard errors (SEs) for DBH, H, and CA ranged from 2.80 to 6.41, 0.43 to 1.63, and 2.87 to 10.24, respectively. In comparison, the results obtained from AdQSM had the mean values of DBH, H, and CA ranging from 35.65 to 51.43 cm, 14.03 to 16.62 m, and 20.82 to 37.88 m^2, respectively. The corresponding SEs for DBH, H, and CA varied from 1.79 to 8.91, 0.44 to 1.64, and 2.89 to

10.4, respectively. Furthermore, large differences were observed in DBH in the specific plots (plot 5 and plot 7) and CA (all plots) while they were nearly identical in H (all plots).

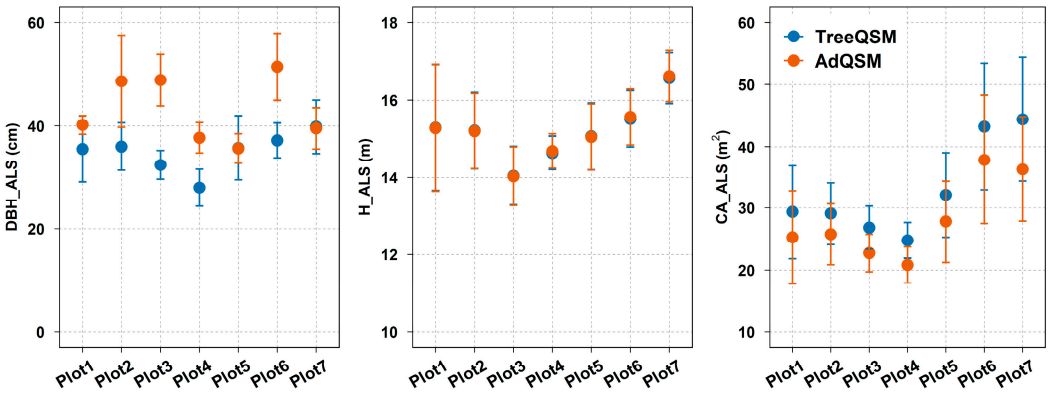

Figure 5. Description of the extracted DBH, H, and CA based on TreeQSM and AdQSM constructed using the ALS point clouds at the plot level.

The comparison of TreeQSM and AdQSM built from ALS for the estimation of DBH, H, and CA at plot level is shown in Figure 6. The TreeQSM and AdQSM exhibited poor performance for estimating DBH, irrespective of TreeQSM (R^2 = 0.35, RMSE = 2.83) and AdQSM (R^2 = 0.12, RMSE = 5.49). However, the association between TreeQSM and AdQSM was strongly linear for the estimation of H with close R^2 values of 0.93 and 0.94, while RMSE values were 0.19 and 0.18. In comparison, the two methods show good performance in the estimation of CA, but AdQSM shows relatively better performance compared with TreeQSM, as AdQSM yielded results with an R^2 of 0.82 and RMSE of 2.57, followed by TreeQSM (R^2 = 0.68, RMSE = 4.09).

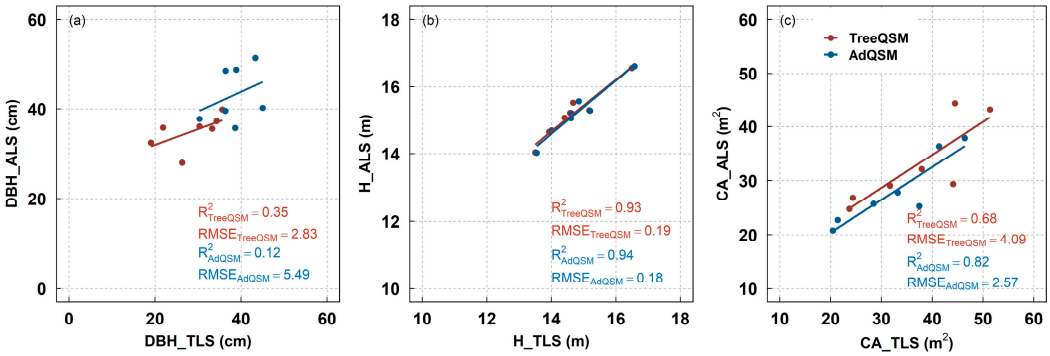

Figure 6. Plot-level comparison of structural metrics (DBH, H, and CA) estimated by TreeQSM and AdQSM methods constructed from TLS and ALS point clouds. (**a**) Estimated DBH comparison between TLS and ALS using two QSMs; (**b**) estimated H comparison between TLS and ALS using two QSMs; (**c**) estimated CA comparison between TLS and ALS using two QSMs.

Further tree-level assessments of DBH, H, and CA estimated from ALS using the TreeQSM and AdQSM methods are shown in Figure 7. Specifically, the distributions of the structural metrics estimated by TreeQSM and AdQSM were skewed. For the TreeQSM results, the estimated DBH, H, and CA ranged from 9.15 to 78.85 cm, 5.72 to 20.27 m, and 4.54 to 144.42 m^2, respectively. The median and mean values for DBH, H, and CA were 29.99 and 32.00 cm (SE: 1.36), 15.00 and 14.42 m (SE: 0.29), and 24.68 and 29.86 m^2 (SE: 2.03), respectively. The estimated CA varied more (CV: 70%) compared with DBH (CV: 44%) and H (CV: 21%). For the AdQSM results, the estimated DBH, H, and CA ranged from 17.88 to 117.96 cm, 5.81 to 20.15 m, and 1.00 to 141.50 m^2, respectively, while the median and mean for DBH, H, and CA were 37.87 and 42.62 cm (SE: 1.75), 15.00 and 14.44 m (SE: 0.29), and

20.00 and 25.09 m^2 (SE: 1.91), respectively. Similar to the TreeQSM results, the estimated CA varied more (CV: 79%) compared with DBH (CV: 42%) and H (CV: 21%). Among the three parameters, the estimated results for H from both methods are very close in terms of distribution and statistical metrics.

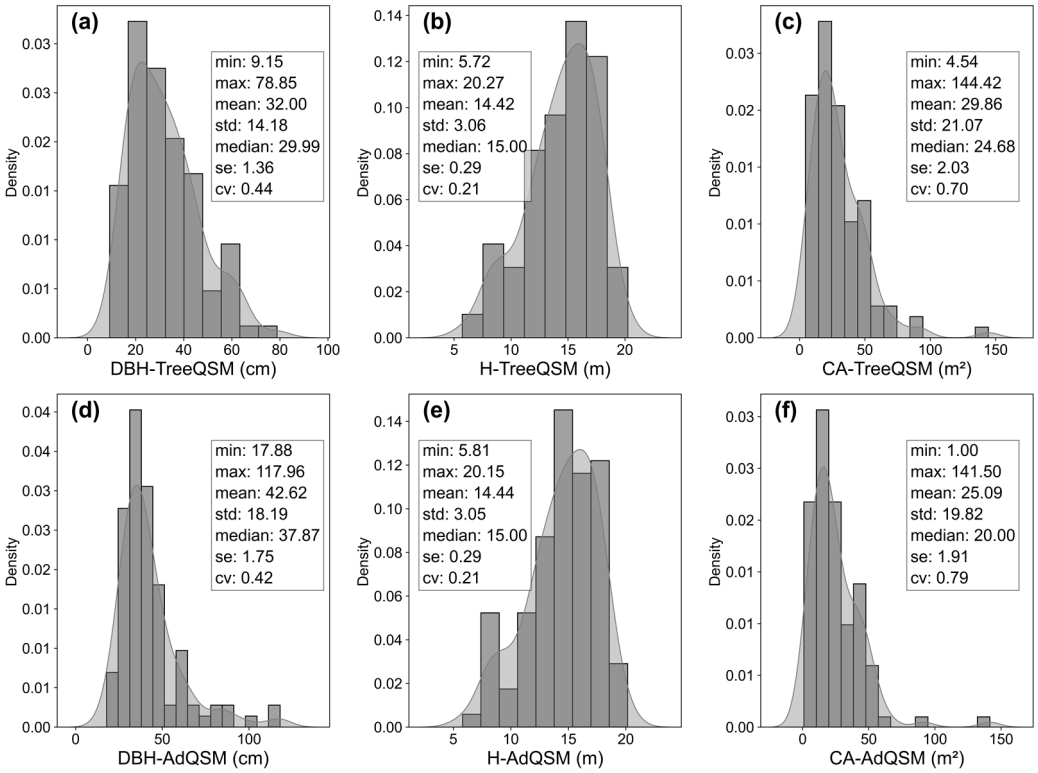

Figure 7. Tree-level distribution of forest metrics (DBH, H, and CA) estimated from ALS data using TreeQSM (**a**–**c**) and AdQSM (**d**–**f**) methods.

The comparison of TreeQSM and AdQSM results derived from ALS for the estimation of DBH, H, and CA at tree level is shown in Figure 8. Similar to the results at the plot level, both methods demonstrated excellent performance in the estimation of H, with the same R^2 of 0.92 and close RMSEs (TreeQSM: 0.82, AdQSM: 0.81). However, both methods still exhibit poor performance in the estimation of DBH, with AdQSM showing the lowest performance (R^2: 0.09; RMSE: 18.22). Although TreeQSM performs relatively better than AdQSM, challenges remain in terms of accuracy (R^2 of 0.40 and RMSE of 11.66). In contrast, both methods yielded acceptable results for the estimation of CA, where the R^2 and RMSE of TreeQSM and AdQSM were 0.71 and 0.76 and 11.79 and 10.37, respectively.

3.2. DAP Point Cloud-Based QSM Estimations: TreeQSM vs. AdQSM

The mean values of DBH ranged from 22.55 to 49.28 cm (SE: 1.80~9.60, Figure 9) for different plots based on TreeQSM, with the highest value occurring in plot 3 (49.28 ± 9.60). Mean DBH values varied from 31.69 to 40.39 cm (SE: 2.60~11.42) from plot 1 to plot 7 based on AdQSM. Significant differences were found between TreeQSM and AdQSM for DBH estimation, except that of plot 6. However, the mean and SE of H in different plots almost overlapped with the ranges of 13.04~16.92 (0.57~1.97) and 13.10~17.06 (0.48~1.94) based on TreeQSM and AdQSM, respectively. The mean CA based on AdQSM (18.13~29.25) was lower than that based on TreeQSM (23.52~33.00) in each plot.

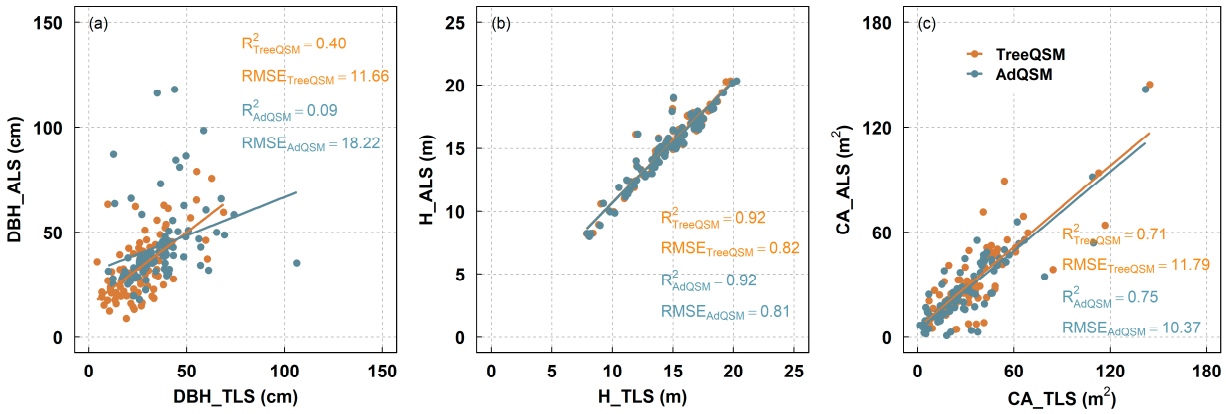

Figure 8. Tree-level comparison of structural metrics (DBH, H, and CA) estimated by TreeQSM and AdQSM methods constructed from TLS and ALS point clouds. (**a**) Estimated DBH comparison between TLS and ALS using two QSMs; (**b**) estimated H comparison between TLS and ALS using two QSMs; (**c**) estimated CA comparison between TLS and ALS using two QSMs.

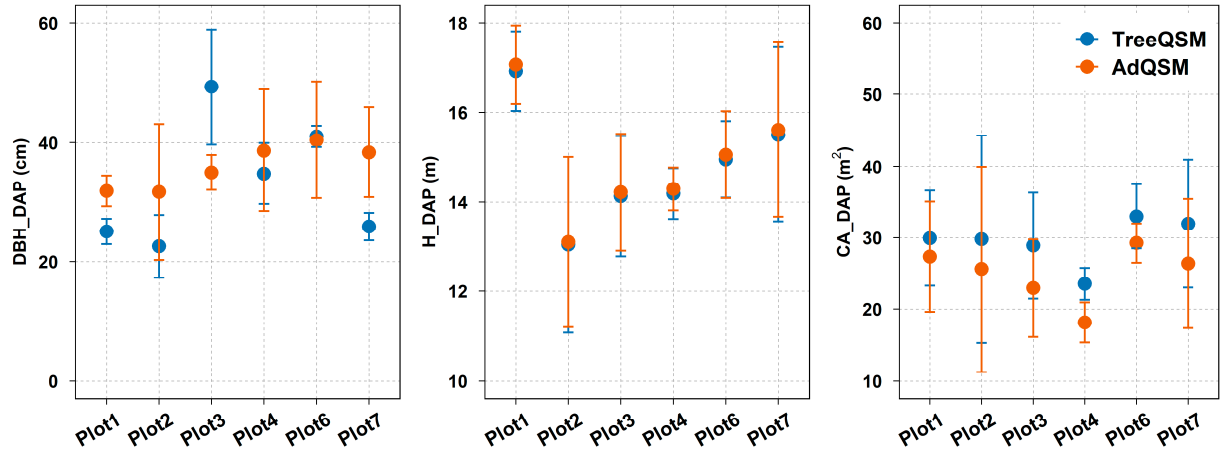

Figure 9. Description of extracted DBH, H, and CA based on the TreeQSM and AdQSM constructed from DAP plot-level point clouds.

The relationships between DAP and TLS based on TreeQSM and AdQSM for DBH, H, and CA are shown in Figure 10. The correlations of DAP and TLS based on TreeQSM and AdQSM showed very low accuracy for DBH, where AdQSM was slightly better than TreeQSM, with higher R^2 and lower RMSE values (R^2: 0.20 vs. 0.00, RMSE: 3.03 vs. 9.62). Moderate performance was found for the CA based on TreeQSM and AdQSM, and AdQSM (R^2: 0.71, RMSE: 1.94) also performed better than TreeQSM (R^2: 0.41, RMSE: 2.31). Nevertheless, it was found that TreeQSM and AdQSM estimated H well, with identical R^2 values of 0.86 and almost identical RMSEs (0.46 vs. 0.47).

The distribution of extracted DBH, H, and CA from TreeQSM and AdQSM constructed using DAP point clouds at the tree level is shown in Figure 11. The DBH ranges were 8.85~91.55 with a mean of 34.16 cm based on TreeQSM and were 10.33~60.76 with a mean of 35.70 cm based on AdQSM. The CV values for DBH from TreeQSM and AdQSM were 47% and 38%, respectively. Similar ranges of H values were observed for TreeQSM (range: 8.64~18.69, mean: 14.63, CV: 20%) and AdQSM (range: 8.71~18.60, mean: 14.73, CV: 19%). A large amplitude of ranges occurred in the CA, with values of 4.58~71.33 (mean: 29.14, CV: 54%) for TreeQSM and of 2.50~67.50 (mean: 24.28, CV: 64%) for AdQSM.

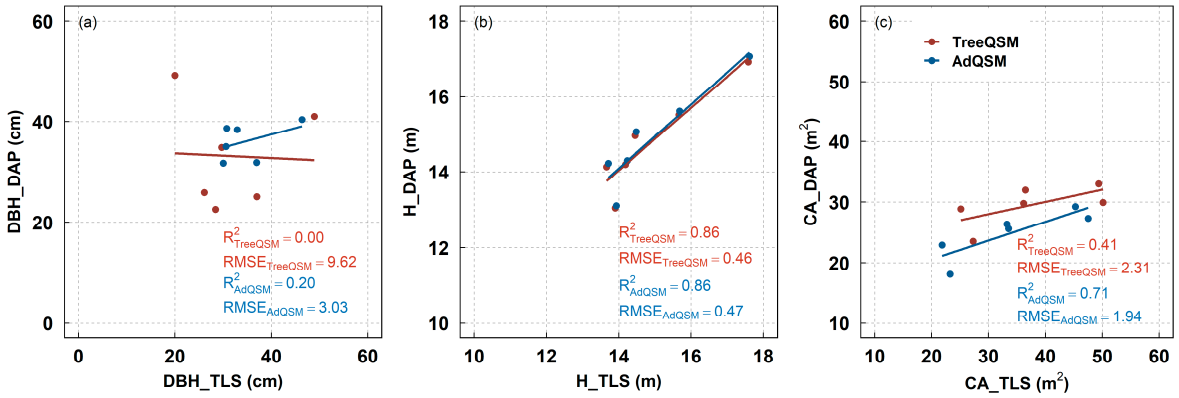

Figure 10. Plot-level comparison of structural metrics (DBH, H, and CA) estimated from TLS and DAP point clouds based on Trees and AdQSM methods. (**a**) Estimated DBH comparison between TLS and DAP using two QSMs; (**b**) estimated H comparison between TLS and DAP using two QSMs; (**c**) estimated CA comparison between TLS and DAP using two QSMs.

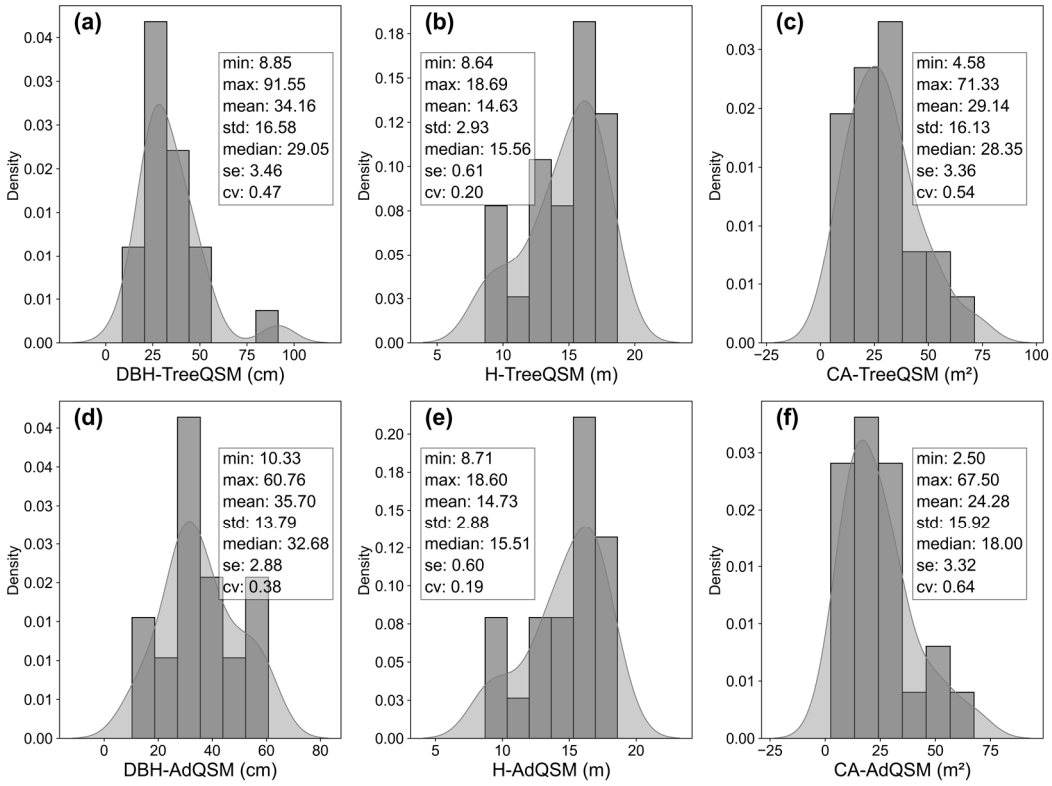

Figure 11. Tree-level distribution of forest metrics (DBH, H, and CA) estimated from DAP data using TreeQSM (**a**–**c**) and AdQSM (**d**–**f**) methods.

At the individual tree level, poor relationships were also found for DBH, regardless of the use of TreeQSM and AdQSM, as indicated by an R^2 lower than 0.03 and RMSE higher than 13.49 (Figure 12a). DAP is closely related to TLS for H, with an R^2 of 0.89 (RMSE: 0.94) for TreeQSM and 0.90 (RMSE: 0.88) for AdQSM (Figure 12b). In addition, DAP displayed a moderate relationship with TLS (Figure 12c), and the TreeQSM had a slightly higher R^2 (0.50 vs. 0.43) and lower RMSE (11.20 vs. 11.80) for the CA when compared with AdQSM.

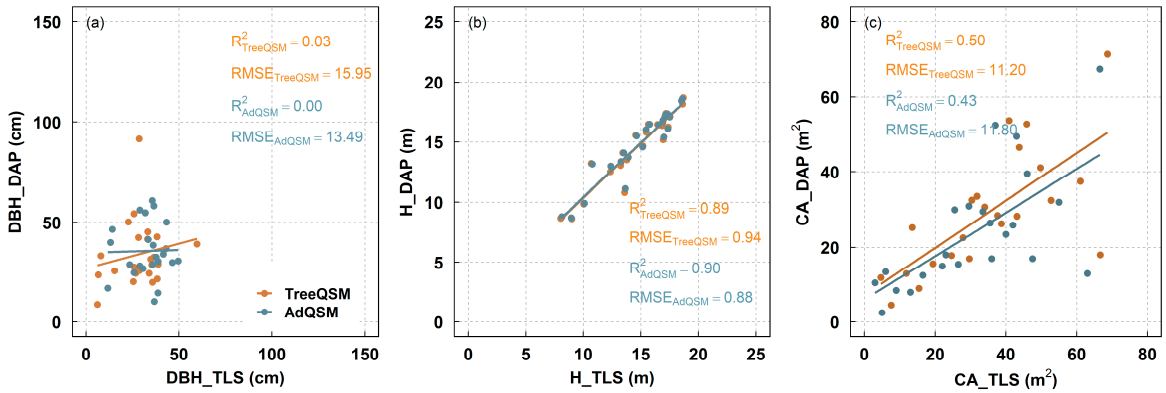

Figure 12. Tree-level comparison of structural metrics (DBH, H, and CA) estimated from TLS and DAP point clouds based on TreeQSM and AdQSM methods. (**a**) Estimated DBH comparison between TLS and DAP using two QSMs; (**b**) estimated H comparison between TLS and DAP using two QSMs; (**c**) estimated CA comparison between TLS and DAP using two QSMs.

4. Discussion

4.1. Accuracy of Estimating Forest Structural Attributes Using Different Point Clouds

Plot-level statistics revealed that ALS-based point clouds provided higher accuracy than DAP-based point clouds for DBH (R^2: 0.12~0.35 vs. 0.00~0.20, RMSE: 2.83~5.49 vs. 3.03~9.62), H (R^2: 0.93~0.94 vs. 0.86~0.86, RMSE: 0.18~0.19 vs. 0.46~0.47), and CA (R^2: 0.68~0.82 vs. 0.41~0.71, RMSE: 2.57~4.09 vs. 1.94~2.31) estimates. Meanwhile, the ALS-based point clouds also behaved better than the DAP-based point clouds did at tree level for DBH (R^2: 0.09~0.40 vs. 0.00~0.03, RMSE: 11.66~18.22 vs. 13.49~15.95), H (R^2: 0.92~0.92 vs. 0.89~0.90, RMSE: 0.81~0.82 vs. 0.88~0.94), and CA (R^2: 0.71~0.75 vs. 0.43~0.50, RMSE: 10.37~11.79 vs. 11.20~11.80) estimations. As a result, the ALS- and DAP-based predictions of forest structural metrics (DBH, H, and CA) with respect to TLS-based point clouds in this study demonstrated that ALS was found to be more accurate than DAP point clouds in a temperate deciduous forest, regardless of plot or tree level.

Our results are consistent with previous studies comparing the accuracy of ALS and DAP point clouds for estimating the most common forest structural metrics [17,21,60,61]. For example, Rahlf et al. [62] obtained the most accurate prediction results for timber volume at both plot and stand levels. Mielcarek et al. [23] observed a lower bias with ALS compared with DAP for estimating tree height in mesic and moist hardwood forests. ALS laser pulses are known to penetrate the forest canopy and characterize the internal structure of the crown, while DAP is limited to describing the outer canopy envelope [19,63]. The current research was conducted in a temperate deciduous forest characterized by complex forest structures, suggesting that ALS is more suitable than DAP for estimating forest structural metrics in complex forests.

4.2. Accuracy of Estimating Forest Structural Metrics between Different QSMs

TreeQSM and AdQSM are state-of-the-art representative tree models and have recently been increasingly used to reconstruct detailed tree models for extracting tree attributes. TreeQSM fits cylinders of each segment segmented from tree point clouds rather than depending on the tree skeleton, while AdQSM fits cylinders based on the extracted complete skeleton [42,48,64]. In several previously reported studies, comparable estimation accuracies between TreeQSM and AdQSM are observed for volume estimation in tropical forests [48] and for stem volume estimation using terrestrial close-range photogrammetry point clouds in a deciduous plantation [65].

This study is the first to evaluate the comparison between TreeQSM and AdQSM constructed from different point clouds in an alpine temperate deciduous forest. The results show that there are no apparent differences in tree height estimates using TreeQSM and AdQSM, regardless of ALS or DAP point clouds, at both plot and tree levels. The

TreeQSM- and AdQSM-derived tree height estimates have been widely reported, and very good performance was achieved in deciduous species [48,65]. However, TreeQSM performed better than AdQSM based on ALS point clouds for estimating DBH, while the opposite was found for estimating crown area. These results indicate that the predictive performance of TreeQSM and AdQSM depends on the determined tree attributes.

4.3. Future Perspectives

In the previously reported studies, the forest structural parameters of tree height and canopy area extracted based on LiDAR data achieved satisfactory results, especially for coniferous forests. However, the estimation accuracy is generally affected by a number of factors, such as site conditions, adjacent vegetation, and understory vegetation. Our results showed promising results for the estimation of forest structural attributes using LiDAR in alpine temperate deciduous forests, while the prediction accuracy still needs to be improved from various perspectives, such as tree segmentation. More tree detection and segmentation approaches for tree information extraction should be further explored in future studies. UAV optical data combined with tree modeling have the potential to provide forest canopy information, while it is challenging to extract forest structural information, so other related methods can be further investigated.

In addition to tree-level information, topographic information such as slope and terrain can also be obtained from remote sensing data. These ALS-derived topological variables could be used for forest phenotyping. The fusion of different remote sensing data sources has been demonstrated to accurately extract forest structural attributes in previous studies [66–68], and a potential future direction would be to assess forest structure in temperate deciduous forests.

5. Conclusions

The ALS-derived forest structural attributes obtained in this study were more closely correlated with those obtained from TLS point clouds, indicating that ALS-based point clouds provide more accurate estimates of forest structural metrics in an alpine temperate deciduous forest. In addition, different QSMs showed little difference for tree height estimates, but behaved differently for DBH and canopy area. LiDAR combined with QSMs appears to be the most efficient and accurate technique for forestry applications, and real-time forest monitoring systems are critical for forest management in the context of climate change.

Author Contributions: Conceptualization, Q.W.; methodology, Q.W. and Y.G.; investigation, Y.G.; formal analysis, Y.G.; writing—original draft preparation, Y.G., G.S. and Q.W. All authors have read and agreed to the published version of the manuscript.

Funding: This research was partly supported by the Japan Society for the Promotion of Science (JSPS) (grant no. 21H02230).

Data Availability Statement: The data are available on reasonable request from the corresponding author.

Acknowledgments: We are grateful to the members of the Laboratory of Macroecology and the Institute of Silviculture, Shizuoka University, for their support with fieldwork. We express our thanks for access to all open-source software and algorithms used in this research.

Conflicts of Interest: The authors declare no conflicts of interest.

References

1. Jurjević, L.; Liang, X.; Gašparović, M.; Balenović, I. Is Field-Measured Tree Height as Reliable as Believed—Part II, A Comparison Study of Tree Height Estimates from Conventional Field Measurement and Low-Cost Close-Range Remote Sensing in a Deciduous Forest. *ISPRS J. Photogramm. Remote Sens.* **2020**, *169*, 227–241. [CrossRef]
2. Luoma, V.; Saarinen, N.; Wulder, M.A.; White, J.C.; Vastaranta, M.; Holopainen, M.; Hyyppä, J. Assessing Precision in Conventional Field Measurements of Individual Tree Attributes. *Forests* **2017**, *8*, 38. [CrossRef]

3. Goodbody, T.R.H.; Coops, N.C.; White, J.C. Digital Aerial Photogrammetry for Updating Area-Based Forest Inventories: A Review of Opportunities, Challenges, and Future Directions. *Curr. For. Rep.* **2019**, *5*, 55–75. [CrossRef]
4. Liang, X.; Kankare, V.; Hyyppä, J.; Wang, Y.; Kukko, A.; Haggrén, H.; Yu, X.; Kaartinen, H.; Jaakkola, A.; Guan, F.; et al. Terrestrial Laser Scanning in Forest Inventories. *ISPRS J. Photogramm. Remote Sens.* **2016**, *115*, 63–77. [CrossRef]
5. White, J.C.; Coops, N.C.; Wulder, M.A.; Vastaranta, M.; Hilker, T.; Tompalski, P. Remote Sensing Technologies for Enhancing Forest Inventories: A Review. *Can. J. Remote Sens.* **2016**, *42*, 619–641. [CrossRef]
6. Filippelli, S.K.; Lefsky, M.A.; Rocca, M.E. Comparison and Integration of Lidar and Photogrammetric Point Clouds for Mapping Pre-Fire Forest Structure. *Remote Sens. Environ.* **2019**, *224*, 154–166. [CrossRef]
7. McNicol, I.M.; Mitchard, E.T.A.; Aquino, C.; Burt, A.; Carstairs, H.; Dassi, C.; Modinga Dikongo, A.; Disney, M.I. To What Extent Can UAV Photogrammetry Replicate UAV LiDAR to Determine Forest Structure? A Test in Two Contrasting Tropical Forests. *J. Geophys. Res. Biogeosci.* **2021**, *126*, e2021JG006586. [CrossRef]
8. Calders, K.; Adams, J.; Armston, J.; Bartholomeus, H.; Bauwens, S.; Bentley, L.P.; Chave, J.; Danson, F.M.; Demol, M.; Disney, M.; et al. Terrestrial Laser Scanning in Forest Ecology: Expanding the Horizon. *Remote Sens. Environ.* **2020**, *251*, 112102. [CrossRef]
9. Weiser, H.; Schäfer, J.; Winiwarter, L.; Krašovec, N.; Fassnacht, F.E.; Höfle, B. Individual Tree Point Clouds and Tree Measurements from Multi-Platform Laser Scanning in German Forests. *Earth Syst. Sci. Data* **2022**, *14*, 2989–3012. [CrossRef]
10. Chamberlain, C.P.; Sánchez Meador, A.J.; Thode, A.E. Airborne Lidar Provides Reliable Estimates of Canopy Base Height and Canopy Bulk Density in Southwestern Ponderosa Pine Forests. *For. Ecol. Manag.* **2021**, *481*, 118695. [CrossRef]
11. Latifi, H.; Fassnacht, F.E.; Müller, J.; Tharani, A.; Dech, S.; Heurich, M. Forest Inventories by LiDAR Data: A Comparison of Single Tree Segmentation and Metric-Based Methods for Inventories of a Heterogeneous Temperate Forest. *Int. J. Appl. Earth Obs. Geoinf.* **2015**, *42*, 162–174. [CrossRef]
12. Shang, C.; Treitz, P.; Caspersen, J.; Jones, T. Estimation of Forest Structural and Compositional Variables Using ALS Data and Multi-Seasonal Satellite Imagery. *Int. J. Appl. Earth Obs. Geoinf.* **2019**, *78*, 360–371. [CrossRef]
13. Yao, W.; Krzystek, P.; Heurich, M. Tree Species Classification and Estimation of Stem Volume and DBH Based on Single Tree Extraction by Exploiting Airborne Full-Waveform LiDAR Data. *Remote Sens. Environ.* **2012**, *123*, 368–380. [CrossRef]
14. Bucksch, A.; Lindenbergh, R.; Abd Rahman, M.Z.; Menenti, M. Breast Height Diameter Estimation from High-Density Airborne LiDAR Data. *IEEE Geosci. Remote Sens. Lett.* **2014**, *11*, 1056–1060. [CrossRef]
15. Kandare, K.; Ørka, H.O.; Chan, J.C.W.; Dalponte, M. Effects of Forest Structure and Airborne Laser Scanning Point Cloud Density on 3D Delineation of Individual Tree Crowns. *Eur. J. Remote Sens.* **2016**, *49*, 337–359. [CrossRef]
16. Richardson, J.J.; Moskal, L.M. Strengths and Limitations of Assessing Forest Density and Spatial Configuration with Aerial LiDAR. *Remote Sens. Environ.* **2011**, *115*, 2640–2651. [CrossRef]
17. Nurminen, K.; Karjalainen, M.; Yu, X.; Hyyppä, J.; Honkavaara, E. Performance of Dense Digital Surface Models Based on Image Matching in the Estimation of Plot-Level Forest Variables. *ISPRS J. Photogramm. Remote Sens.* **2013**, *83*, 104–115. [CrossRef]
18. Nyamgeroh, B.B.; Groen, T.A.; Weir, M.J.C.; Dimov, P.; Zlatanov, T. Detection of Forest Canopy Gaps from Very High Resolution Aerial Images. *Ecol. Indic.* **2018**, *95*, 629–636. [CrossRef]
19. White, J.C.; Wulder, M.A.; Vastaranta, M.; Coops, N.C.; Pitt, D.; Woods, M. The Utility of Image-Based Point Clouds for Forest Inventory: A Comparison with Airborne Laser Scanning. *Forests* **2013**, *4*, 518–536. [CrossRef]
20. White, J.C.; Stepper, C.; Tompalski, P.; Coops, N.C.; Wulder, M.A. Comparing ALS and Image-Based Point Cloud Metrics and Modelled Forest Inventory Attributes in a Complex Coastal Forest Environment. *Forests* **2015**, *6*, 3704–3732. [CrossRef]
21. Gobakken, T.; Bollandsås, O.M.; Næsset, E. Comparing Biophysical Forest Characteristics Estimated from Photogrammetric Matching of Aerial Images and Airborne Laser Scanning Data. *Scand. J. For. Res.* **2015**, *30*, 73–86. [CrossRef]
22. Cao, L.; Liu, H.; Fu, X.; Zhang, Z.; Shen, X.; Ruan, H. Comparison of UAV LiDAR and Digital Aerial Photogrammetry Point Clouds for Estimating Forest Structural Attributes in Subtropical Planted Forests. *Forests* **2019**, *10*, 145. [CrossRef]
23. Mielcarek, M.; Kamińska, A.; Stereńczak, K. Digital Aerial Photogrammetry (DAP) and Airborne Laser Scanning (ALS) as Sources of Information about Tree Height: Comparisons of the Accuracy of Remote Sensing Methods for Tree Height Estimation. *Remote Sens.* **2020**, *12*, 1808. [CrossRef]
24. Disney, M. Terrestrial LiDAR: A Three-Dimensional Revolution in How We Look at Trees. *New Phytol.* **2019**, *222*, 1736–1741. [CrossRef] [PubMed]
25. Liu, J.; Wang, T.; Skidmore, A.K.; Jones, S.; Heurich, M.; Beudert, B.; Premier, J. Comparison of Terrestrial LiDAR and Digital Hemispherical Photography for Estimating Leaf Angle Distribution in European Broadleaf Beech Forests. *ISPRS J. Photogramm. Remote Sens.* **2019**, *158*, 76–89. [CrossRef]
26. Saarinen, N.; Kankare, V.; Vastaranta, M.; Luoma, V.; Pyörälä, J.; Tanhuanpää, T.; Liang, X.; Kaartinen, H.; Kukko, A.; Jaakkola, A.; et al. Feasibility of Terrestrial Laser Scanning for Collecting Stem Volume Information from Single Trees. *ISPRS J. Photogramm. Remote Sens.* **2017**, *123*, 140–158. [CrossRef]
27. Terryn, L.; Calders, K.; Bartholomeus, H.; Bartolo, R.E.; Brede, B.; D'hont, B.; Disney, M.; Herold, M.; Lau, A.; Shenkin, A.; et al. Quantifying Tropical Forest Structure through Terrestrial and UAV Laser Scanning Fusion in Australian Rainforests. *Remote Sens. Environ.* **2022**, *271*, 112912. [CrossRef]
28. Hancock, S.; Anderson, K.; Disney, M.; Gaston, K.J. Measurement of Fine-Spatial-Resolution 3D Vegetation Structure with Airborne Waveform Lidar: Calibration and Validation with Voxelised Terrestrial Lidar. *Remote Sens. Environ.* **2017**, *188*, 37–50. [CrossRef]

29. Hopkinson, C.; Lovell, J.; Chasmer, L.; Jupp, D.; Kljun, N.; van Gorsel, E. Integrating Terrestrial and Airborne Lidar to Calibrate a 3D Canopy Model of Effective Leaf Area Index. *Remote Sens. Environ.* **2013**, *136*, 301–314. [CrossRef]
30. Béland, M.; Baldocchi, D.D.; Widlowski, J.L.; Fournier, R.A.; Verstraete, M.M. On Seeing the Wood from the Leaves and the Role of Voxel Size in Determining Leaf Area Distribution of Forests with Terrestrial LiDAR. *Agric. For. Meteorol.* **2014**, *184*, 82–97. [CrossRef]
31. Hosoi, F.; Nakai, Y.; Omasa, K. 3-D Voxel-Based Solid Modeling of a Broad-Leaved Tree for Accurate Volume Estimation Using Portable Scanning Lidar. *ISPRS J. Photogramm. Remote Sens.* **2013**, *82*, 41–48. [CrossRef]
32. Popescu, S.C.; Zhao, K. A Voxel-Based Lidar Method for Estimating Crown Base Height for Deciduous and Pine Trees. *Remote Sens. Environ.* **2008**, *112*, 767–781. [CrossRef]
33. Côté, J.F.; Widlowski, J.L.; Fournier, R.A.; Verstraete, M.M. The Structural and Radiative Consistency of Three-Dimensional Tree Reconstructions from Terrestrial Lidar. *Remote Sens. Environ.* **2009**, *113*, 1067–1081. [CrossRef]
34. Hackenberg, J.; Morhart, C.; Sheppard, J.; Spiecker, H.; Disney, M. Highly Accurate Tree Models Derived from Terrestrial Laser Scan Data: A Method Description. *Forests* **2014**, *5*, 1069–1105. [CrossRef]
35. Grau, E.; Durrieu, S.; Fournier, R.; Gastellu-Etchegorry, J.P.; Yin, T. Estimation of 3D Vegetation Density with Terrestrial Laser Scanning Data Using Voxels. A Sensitivity Analysis of Influencing Parameters. *Remote Sens. Environ.* **2017**, *191*, 373–388. [CrossRef]
36. Xu, Y.; Tong, X.; Stilla, U. Voxel-Based Representation of 3D Point Clouds: Methods, Applications, and Its Potential Use in the Construction Industry. *Autom. Constr.* **2021**, *126*, 103675. [CrossRef]
37. Nguyen, V.T.; Fournier, R.A.; Côté, J.F.; Pimont, F. Estimation of Vertical Plant Area Density from Single Return Terrestrial Laser Scanning Point Clouds Acquired in Forest Environments. *Remote Sens. Environ.* **2022**, *279*, 113115. [CrossRef]
38. Putman, E.B.; Popescu, S.C.; Eriksson, M.; Zhou, T.; Klockow, P.; Vogel, J.; Moore, G.W. Detecting and Quantifying Standing Dead Tree Structural Loss with Reconstructed Tree Models Using Voxelized Terrestrial Lidar Data. *Remote Sens. Environ.* **2018**, *209*, 52–65. [CrossRef]
39. Pimont, F.; Allard, D.; Soma, M.; Dupuy, J.L. Estimators and Confidence Intervals for Plant Area Density at Voxel Scale with T-LiDAR. *Remote Sens. Environ.* **2018**, *215*, 343–370. [CrossRef]
40. Wang, C.; Luo, S.; Xi, X.; Nie, S.; Ma, D.; Huang, Y. Influence of Voxel Size on Forest Canopy Height Estimates Using Full-Waveform Airborne LiDAR Data. *For. Ecosyst.* **2020**, *7*, 31. [CrossRef]
41. Brede, B.; Calders, K.; Lau, A.; Raumonen, P.; Bartholomeus, H.M.; Herold, M.; Kooistra, L. Non-Destructive Tree Volume Estimation through Quantitative Structure Modelling: Comparing UAV Laser Scanning with Terrestrial LIDAR. *Remote Sens. Environ.* **2019**, *233*, 111355. [CrossRef]
42. Raumonen, P.; Kaasalainen, M.; Markku, Å.; Kaasalainen, S.; Kaartinen, H.; Vastaranta, M.; Holopainen, M.; Disney, M.; Lewis, P. Fast Automatic Precision Tree Models from Terrestrial Laser Scanner Data. *Remote Sens.* **2013**, *5*, 491–520. [CrossRef]
43. Gonzalez de Tanago, J.; Lau, A.; Bartholomeus, H.; Herold, M.; Avitabile, V.; Raumonen, P.; Martius, C.; Goodman, R.C.; Disney, M.; Manuri, S.; et al. Estimation of Above-Ground Biomass of Large Tropical Trees with Terrestrial LiDAR. *Methods Ecol. Evol.* **2018**, *9*, 223–234. [CrossRef]
44. Lau, A.; Bentley, L.P.; Martius, C.; Shenkin, A.; Bartholomeus, H.; Raumonen, P.; Malhi, Y.; Jackson, T.; Herold, M. Quantifying Branch Architecture of Tropical Trees Using Terrestrial LiDAR and 3D Modelling. *Trees—Struct. Funct.* **2018**, *32*, 1219–1231. [CrossRef]
45. Terryn, L.; Calders, K.; Disney, M.; Origo, N.; Malhi, Y.; Newnham, G.; Raumonen, P.; Åkerblom, M.; Verbeeck, H. Tree Species Classification Using Structural Features Derived from Terrestrial Laser Scanning. *ISPRS J. Photogramm. Remote Sens.* **2020**, *168*, 170–181. [CrossRef]
46. Wilkes, P.; Disney, M.; Vicari, M.B.; Calders, K.; Burt, A. Estimating Urban above Ground Biomass with Multi-Scale LiDAR. *Carbon Balance Manag.* **2018**, *13*, 10. [CrossRef]
47. Hackenberg, J.; Spiecker, H.; Calders, K.; Disney, M.; Raumonen, P. SimpleTree—An Efficient Open Source Tool to Build Tree Models from TLS Clouds. *Forests* **2015**, *6*, 4245–4294. [CrossRef]
48. Fan, G.; Nan, L.; Dong, Y.; Su, X.; Chen, F. AdQSM: A New Method for Estimating above-Ground Biomass from TLS Point Clouds. *Remote Sens.* **2020**, *12*, 3089. [CrossRef]
49. Krishna Moorthy, S.M.; Raumonen, P.; Van den Bulcke, J.; Calders, K.; Verbeeck, H. Terrestrial Laser Scanning for Non-Destructive Estimates of Liana Stem Biomass. *For. Ecol. Manag.* **2020**, *456*, 117751. [CrossRef]
50. Åkerblom, M.; Kaitaniemi, P. Terrestrial Laser Scanning: A New Standard of Forest Measuring and Modelling? *Ann. Bot.* **2021**, *128*, 653–661. [CrossRef]
51. Bienert, A.; Georgi, L.; Kunz, M.; Maas, H.G.; von Oheimb, G. Comparison and Combination of Mobile and Terrestrial Laser Scanning for Natural Forest Inventories. *Forests* **2018**, *9*, 395. [CrossRef]
52. Calders, K.; Newnham, G.; Burt, A.; Murphy, S.; Raumonen, P.; Herold, M.; Culvenor, D.; Avitabile, V.; Disney, M.; Armston, J.; et al. Nondestructive Estimates of Above-Ground Biomass Using Terrestrial Laser Scanning. *Methods Ecol. Evol.* **2015**, *6*, 198–208. [CrossRef]
53. Jackson, T.; Shenkin, A.; Wellpott, A.; Calders, K.; Origo, N.; Disney, M.; Burt, A.; Raumonen, P.; Gardiner, B.; Herold, M.; et al. Finite Element Analysis of Trees in the Wind Based on Terrestrial Laser Scanning Data. *Agric. For. Meteorol.* **2019**, *265*, 137–144. [CrossRef]

54. Ye, N.; van Leeuwen, L.; Nyktas, P. Analysing the Potential of UAV Point Cloud as Input in Quantitative Structure Modelling for Assessment of Woody Biomass of Single Trees. *Int. J. Appl. Earth Obs. Geoinf.* **2019**, *81*, 47–57. [CrossRef]
55. Song, G.M.; Wang, Q.; Jin, J. Leaf Photosynthetic Capacity of Sunlit and Shaded Mature Leaves in a Deciduous Forest. *Forests* **2020**, *11*, 318. [CrossRef]
56. Wang, Q.; Putri, N.A.; Gan, Y.; Song, G.M. Combining Both Spectral and Textural Indices for Alleviating Saturation Problem in Forest LAI Estimation Using Sentinel-2 Data. *Geocarto Int.* **2022**, *37*, 10511–10531. [CrossRef]
57. Wang, X.; Yang, Z.; Cheng, X.; Stoter, J.; Xu, W.; Wu, Z.; Nan, L. GlobalMatch: Registration of Forest Terrestrial Point Clouds by Global Matching of Relative Stem Positions. *ISPRS J. Photogramm. Remote Sens.* **2023**, *197*, 71–86. [CrossRef]
58. Hackenberg, J.; Calders, K.; Miro, D.; Raumonen, P.; Piboule, A.; Mathias, D. SimpleForest—A Comprehensive Tool for 3d Reconstruction of Trees from Forest Plot Point Clouds. *bioRxiv* **2021**. [CrossRef]
59. Du, S.; Lindenbergh, R.; Ledoux, H.; Stoter, J.; Nan, L. AdTree: Accurate, Detailed, and Automatic Modelling of Laser-Scanned Trees. *Remote Sens.* **2019**, *11*, 2074. [CrossRef]
60. Järnstedt, J.; Pekkarinen, A.; Tuominen, S.; Ginzler, C.; Holopainen, M.; Viitala, R. Forest Variable Estimation Using a High-Resolution Digital Surface Model. *ISPRS J. Photogramm. Remote Sens.* **2012**, *74*, 78–84. [CrossRef]
61. Noordermeer, L.; Bollandsås, O.M.; Ørka, H.O.; Næsset, E.; Gobakken, T. Comparing the Accuracies of Forest Attributes Predicted from Airborne Laser Scanning and Digital Aerial Photogrammetry in Operational Forest Inventories. *Remote Sens. Environ.* **2019**, *226*, 26–37. [CrossRef]
62. Rahlf, J.; Breidenbach, J.; Solberg, S.; Næsset, E.; Astrup, R. Comparison of Four Types of 3D Data for Timber Volume Estimation. *Remote Sens. Environ.* **2014**, *155*, 325–333. [CrossRef]
63. White, J.C.; Tompalski, P.; Coops, N.C.; Wulder, M.A. Comparison of Airborne Laser Scanning and Digital Stereo Imagery for Characterizing Forest Canopy Gaps in Coastal Temperate Rainforests. *Remote Sens. Environ.* **2018**, *208*, 1–14. [CrossRef]
64. Li, J.; Wu, H.; Xiao, Z.; Lu, H. 3D Modeling of Laser-Scanned Trees Based on Skeleton Refined Extraction. *Int. J. Appl. Earth Obs. Geoinf.* **2022**, *112*, 102943. [CrossRef]
65. Dong, Y.; Fan, G.; Zhou, Z.; Liu, J.; Wang, Y.; Chen, F. Low Cost Automatic Reconstruction of Tree Structure by Adqsm with Terrestrial Close-Range Photogrammetry. *Forests* **2021**, *12*, 1020. [CrossRef]
66. Dai, W.; Yang, B.; Liang, X.; Dong, Z.; Huang, R.; Wang, Y.; Li, W. Automated Fusion of Forest Airborne and Terrestrial Point Clouds through Canopy Density Analysis. *ISPRS J. Photogramm. Remote Sens.* **2019**, *156*, 94–107. [CrossRef]
67. Guo, L.; Wu, Y.; Deng, L.; Hou, P.; Zhai, J.; Chen, Y. A Feature-Level Point Cloud Fusion Method for Timber Volume of Forest Stands Estimation. *Remote Sens.* **2023**, *15*, 2995. [CrossRef]
68. Paris, C.; Kelbe, D.; Van Aardt, J.; Bruzzone, L. A Novel Automatic Method for the Fusion of ALS and TLS LiDAR Data for Robust Assessment of Tree Crown Structure. *IEEE Trans. Geosci. Remote Sens.* **2017**, *55*, 3679–3693. [CrossRef]